

## Crystalline structure in aliphatic polyketones

J.M. Lagaron<sup>a,\*</sup>, M.E. Vickers<sup>b</sup>, A.K. Powell<sup>a</sup>, N.S. Davidson<sup>a</sup>

<sup>a</sup>BP Chemicals, Applied Technology, P.O. Box 21, Bo'ness Road, Grangemouth, Stirlingshire, Scotland, FK3 9XH, UK

<sup>b</sup>Department of Materials Science and Metallurgy, University of Cambridge, Pembroke Street, Cambridge CB2 3QZ, UK

Received 15 April 1999; received in revised form 22 June 1999; accepted 24 June 1999

### Abstract

The crystalline structure of a number of perfectly 1:1 alternating  $\alpha$ -olefin:carbon monoxide aliphatic polyketones produced by the polymerisation of ethene with carbon monoxide (ECO polymers) and mixtures of ethene and propene with carbon monoxide (EPCO polymers) have been studied by wide angle X-ray scattering (WAXS), Raman spectroscopy and differential scanning calorimetry (DSC). It is further confirmed that both WAXS and Raman spectroscopy are suitable techniques for the characterisation of the two polymorphs ( $\alpha$  and  $\beta$ ) reported for these materials. DSC detected the presence of small endotherms around 100°C associated with the transition from the  $\alpha$  to the  $\beta$  phase only in the ECO material. In accordance with previous work, it is found that the  $\alpha/\beta$  ratio is the highest for the ECO polymer and decreases with increasing propene content in EPCO polymers. Above 2.9 mol% of propene incorporation, EPCO polymers show exclusively  $\beta$  phase. Heat of fusion (degree of crystallinity) and melting point decreased with increasing propene level, as expected. Accordingly, crystalline density (as determined by WAXS) and lattice interchain interaction (as determined by Raman) were also found to decrease by increasing the propene incorporation. © 2000 Elsevier Science Ltd. All rights reserved.

**Keywords:** Aliphatic polyketones; Raman spectroscopy; Wide angle X-ray scattering

### 1. Introduction

Aliphatic polyketones are a family of polymers prepared by the polymerisation of  $\alpha$ -olefins and carbon monoxide in a perfectly 1:1 alternating sequence using palladium catalysts [1,2]. These polymers are semi-crystalline thermoplastics and are reported to have a useful combination of mechanical, high temperature, chemical resistance, wear resistance and barrier properties giving them significant commercial potential in a broad range of engineering, barrier packaging, fibre and blend applications [3,4].

The simplest aliphatic polyketone is the polymer of ethene and carbon monoxide. It can be regarded as a homopolymer of the repeat unit  $-(\text{CH}_2-\text{CH}_2-\text{C}=\text{O})-$ . It has a crystalline melting point typically between 255 and 260°C. Lower melting point polymers can be produced by the incorporation of propene in addition to ethene. The aliphatic polyketones derived from a mixture of ethene, propene and carbon monoxide can be regarded as random copolymers of  $-(\text{CH}_2-\text{CH}_2-\text{C}=\text{O})-$  and  $-(\text{CH}_2-\text{CH}(\text{CH}_3)-\text{C}=\text{O})-$  units. For brevity, throughout this paper, aliphatic polyketones derived from ethene and carbon monoxide will be designated ECO and those derived from ethene, propene and carbon monoxide will be designated EPCO.

The original crystalline morphology that Chatani et al. [5,6] determined for polyketone is directly analogous to the unit cell of polyethylene, space group *Pnam* (No. 62) but with the *c*-axis increased by three times to account for the carbonyl group. More recently, Lommerts et al. and Klop et al. [7,8] reported a denser phase in polyketones. It has the same space group No. 62 but a different setting *Pbnm*. They designated this denser phase (density 1.383 g cm<sup>-3</sup>) alpha ( $\alpha$ ) and the original Chatani structure (density 1.297 g cm<sup>-3</sup>) beta ( $\beta$ ). Both crystalline structures have two polymer chains in an all-*trans* conformation along the *c*-axis, but differ in the mode of chain packing. In the  $\alpha$  form the carbonyl groups are closer together than in the  $\beta$  one. Also, the angle between the molecular plane and the *bc* plane is 26° for the  $\alpha$  form whereas it is 40° for the  $\beta$  form. The crystalline form favoured strongly depends on polymer composition, but also on other factors like temperature, applied stress and kinetic factors. The  $\alpha$  form, thought to arise from highly efficient dipolar intermolecular interaction within the lattice, has been reported in well-oriented perfectly alternating polymers of ethene and carbon monoxide (ECO). The  $\beta$  form is exclusive in ethene/propene/carbon monoxide (EPCO) polymers above 2.5 mol% of propene. A phase change from  $\alpha$  to  $\beta$  form occurs in oriented fibers at temperatures between 110 and 125°C whereas the processes of spinning and drawing leads to

\* Corresponding author.

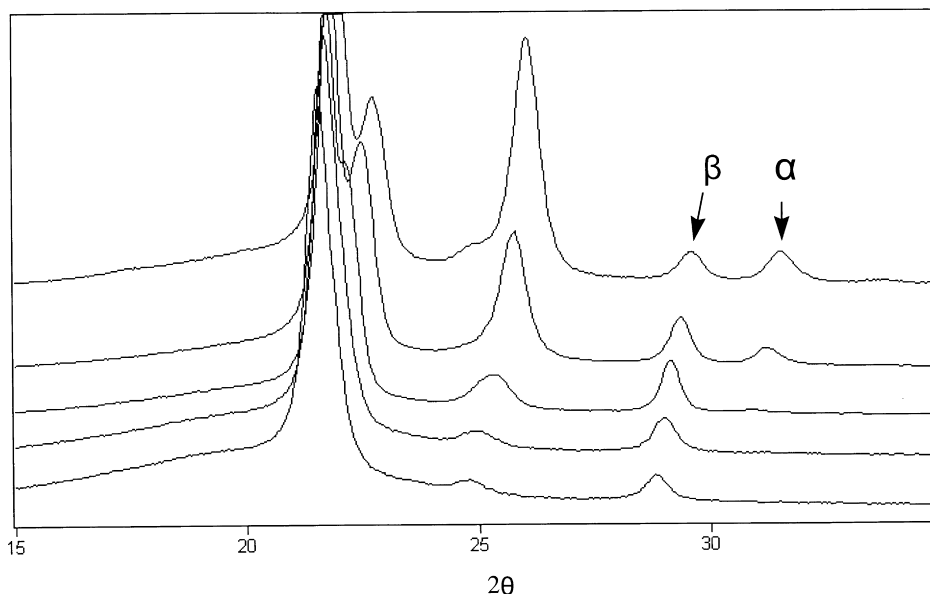


Fig. 1. WAXS curves of, from top to bottom, ECO, EPCO(1.2), EPCO(2.9), EPCO(4.6), EPCO(7.2).

the transformation of the unoriented  $\beta$ -rich symmetry into oriented  $\alpha$ -rich symmetry [7,8].

Raman spectroscopy characterisation of a range of ex-reactor aliphatic polyketones (ECO and EPCO materials) powders, revealed spectral differences in the  $-\text{CH}_2-$  bending region [9]. These differences were attributed to factor group splitting arising from the different polymorphs described above. The results suggested that ECO polymers show a crystalline structure made of a mixture of  $\alpha$  and  $\beta$  forms. On the other hand, the EPCO polymers predominantly show a  $\beta$  phase crystalline structure.

In the current study, wide angle X-ray scattering (WAXS) data and the crystalline density, calculated from cell parameters, are compared with Raman spectroscopy and DSC results. A unified description of the crystalline structure in terms of the above crystalline polymorphism is provided.

## 2. Experimental

### 2.1. Materials

The aliphatic polyketones, ECO and EPCO, used in this study were synthesised at BP Chemicals using a proprietary catalyst. The polymer powder was used as received from the production process.

Films of 150  $\mu\text{m}$  thickness were compression moulded at a temperature above the melting point, using an electrically heated hydraulic press and cooled under pressure at 15°C/min to room temperature.

The mol% of propene in EPCO polymers, as measured by  $^1\text{H}$  NMR, is given in parenthesis attached to the code EPCO throughout the paper. As an example, EPCO(2.9) designates a polymer comprising 2.9 mol% of propene, 47.1 mol% of

ethene and 50 mol% of carbon monoxide. The typical weight average molecular weight ( $M_w$ ) determined by gel permeation chromatography is around 130 000 relative to PMMA standards and the polydispersity index is around two.

### 2.2. Raman equipment

The spectra were recorded with a Raman system [10] comprising of a JY THR1000 single monochromator, Wright instruments CCD camera, Ti sapphire laser at 752 nm, with a Kaiser holographic edge filter. Typically 50 mW of laser light was used at the sample with a 20 $\times$  long distance microscope objective. Integration times were around 20 s and the spectral resolution is 3  $\text{cm}^{-1}$ .

The curve-fitting of the Raman experimental profiles was carried out with the GRAMS Research 2000 software package from Galactic industries. Voigt (convolution of Lorentzian and Gaussian) profiles, no-restrictions and linear baseline conditions were utilised. From this, band areas and band positions were derived.

### 2.3. Wide angle X-ray scattering

The X-ray data were obtained with a Bruker D500 diffractometer operating in reflection mode. The thin polymer films ( $\approx 0.11$ – $0.26$  mm) were mounted on a single crystal silicon substrate. The data were fitted, with pseudo-Voigt functions, using the Philips program PROFIT to determine peak positions, intensities, widths and areas [11]. The peak positions were corrected for absorption into the sample by using the following formula by Vonk and Wilson [12,13]

$$\Delta 2\theta(\text{radians}) = -\frac{\sin 2\theta}{2\mu R} - \frac{2t \cos \theta}{R(e^{2\mu t \csc \theta} - 1)}$$

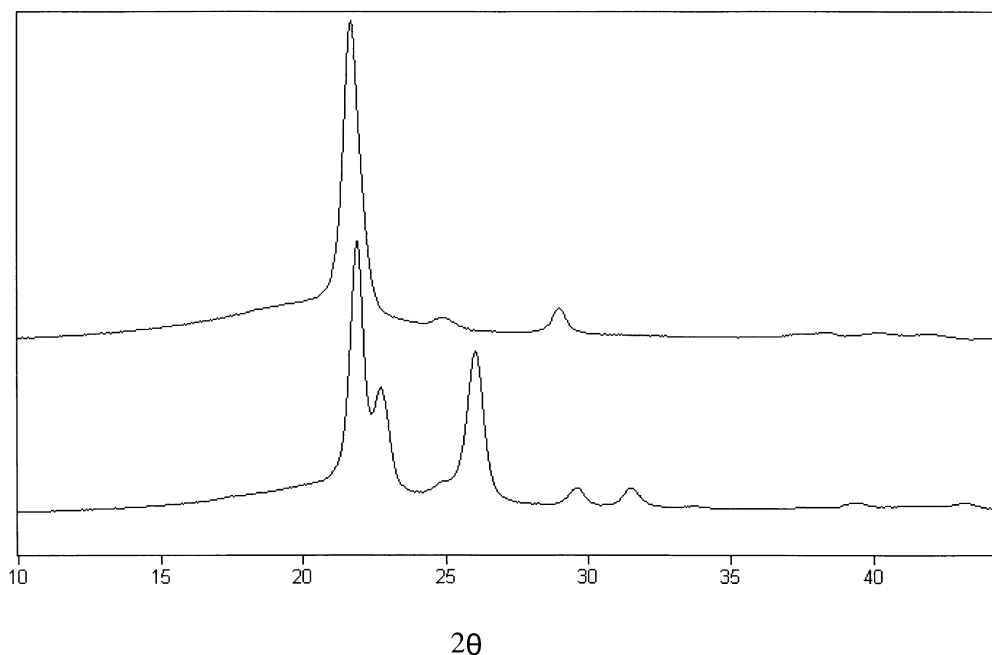


Fig. 2. Full WAXS pattern of (top) EPCO(4.6) showing only  $\beta$  phase and (bottom) ECO showing the largest content in the  $\alpha$  form.

where  $R$  is the radius of the diffractometer,  $t$  the sample thickness and  $\mu$  the linear absorption coefficient.

The cell parameters were determined by a least squares fit to 7–10 reflections using the Bruker program APPLEMAN. Well resolved reflections were given a high weighting and the very weak or poorly resolved ones a low weighting in the fitting procedure. In several instances there was a lack of strong reflections with an index of one, thus the value for the  $c$  cell parameter has not really been determined but rather allowed to refine using as input the literature value. Crystalline densities ( $\rho_c$ ) have been calculated from the experimental cell parameters using the following equation and assuming that the unit cell contains just two polyketone chains

$$\rho_c = ZM/VN$$

where  $Z$  is the number of molecules per unit cell,  $M$  the

molecular weight,  $V$  the unit cell volume and  $N$  the Avogadro number.

#### 2.4. Differential scanning calorimetry

Differential scanning calorimetry (DSC) curves were recorded in a Perkin–Elmer DSC 7 calorimeter at a heating speed of 10°C/min from 0 to 270°C on typically 4 mg of sample cut from the same films used for WAXS measurements. The calibration of the DSC was carried out with standard samples of indium and tin.

### 3. Results and discussions

#### 3.1. WAXS and DSC experiments

The WAXS curves of some polyketone samples are shown in Fig. 1. The major differences between samples

Table 1

Ranking of  $\alpha$  phase content as estimated by both the WAXS area ratio  $I_{31}/I_{29}^\circ$  and the Raman area ratio  $I_{1440}/I_{C=O}$  (both ratios are normalised to one by dividing the ratios between that of the ECO sample), the crystalline density by WAXS and lattice parameters, and the Raman  $-\text{CH}_2-$  bending splitting separation for the different samples

Sample	WAXS $I_{31}/I_{29}$	Raman $I_{1440}/I_{C=O}$	Crystalline density ( $\text{g}/\text{cm}^3$ )	Lattice parameters ( $\text{\AA}$ )			$-\text{CH}_2-$ splitting separation ( $\text{cm}^{-1}$ )
				$a$	$b$	$c$	
ECO	1	1	1.402( $\alpha$ )	6.88	5.01	7.60	25.2( $\alpha$ )
			1.328( $\beta$ )	7.80	4.74	7.58	15.2( $\beta$ )
EPCO(1.2)	0.4	0.6	1.301( $\beta$ )	7.90	4.76	7.61	24.0( $\alpha$ ), 14.7( $\beta$ )
EPCO(2.9)	0.07	0.01	1.287( $\beta$ )	7.99	4.76	7.60	13.3( $\beta$ )
EPCO(5.1)	0	0	1.274( $\beta$ )	8.08	4.75	7.61	13.4( $\beta$ )
EPCO(7.2)	0	0	1.258( $\beta$ )	8.15	4.76	7.62	11.4( $\beta$ )

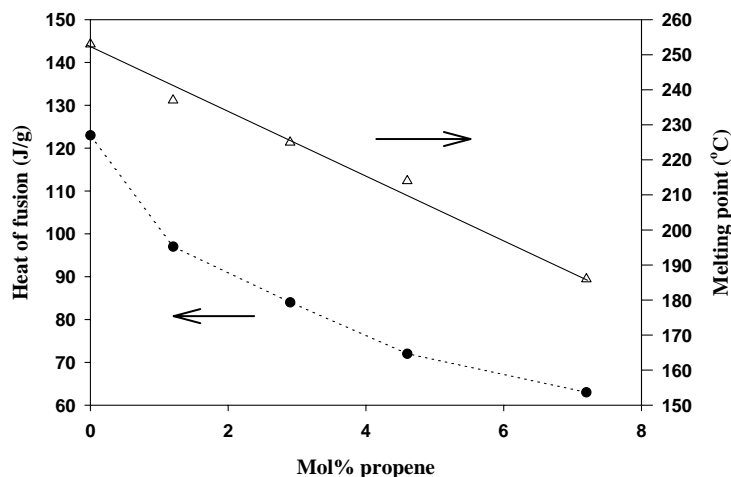


Fig. 3. Melting point (maximum of melting) and heat of fusion as determined by DSC at 10°C/min as a function of propene incorporation.

arose from variations in the ratio of the  $\alpha$  and  $\beta$  phase and minor differences from changes in the crystallinity and cell parameters. A comprehensive description of the WAXS peak assignments and of modelling work leading to the characterisation of the two-polymorph lattices is given in Refs. [5–8]. The differences between the  $\alpha$  and  $\beta$  phases are highlighted in Fig. 2, which shows the WAXS patterns of two extreme samples in terms of crystalline polymorphism. The bottom curve is believed to show a high content of  $\alpha$  phase, whereas the top curve only shows  $\beta$  phase peaks. In this study, we have used the peak at an angle of 31°, attributed to the plane  $\alpha$  (210), to characterise the  $\alpha$  phase and the peak at an angle of 29°, attributed to the plane  $\beta$  (210), to characterise the  $\beta$  phase. Both peaks can be easily quantified by curve-fitting of the experimental data, as they do not overlap with other peaks. Fig. 1 shows that the peak at 31° (assigned to the  $\alpha$  phase) has the largest intensity for the ECO sample closely followed by EPCO(1.2). In the WAXS curves of the other EPCO materials (above 1.2 mol% of propene) this reflection is very weak or not at all present. The first column of Table 1 shows the ratio of the areas of WAXS peaks at 31 and at 29° for the different samples. This

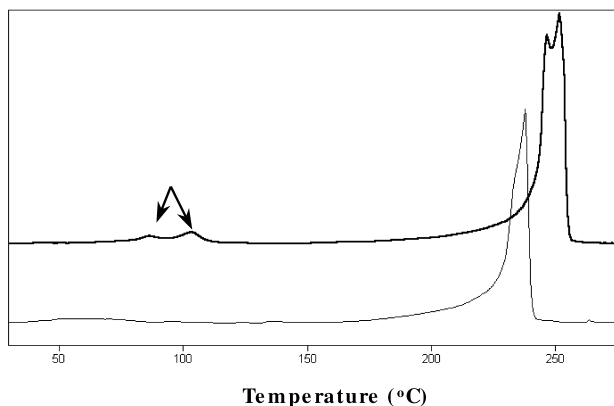


Fig. 4. DSC endotherms for, from top to bottom, ECO and EPCO(1.2). The arrows indicate the  $\alpha$  to  $\beta$  phase transition endotherms.

corresponds to the ratio of the  $\alpha$  to  $\beta$  phase content for the various samples. ECO has the largest proportion of  $\alpha$  crystals, and this decreases with increasing the level of propene incorporation in EPCO samples. For samples above 2.9% of propene content the  $\alpha$  phase is absent and the crystalline morphology is exclusively made of  $\beta$  phase.

Melting point and heat of fusion were determined by DSC and are plotted in Fig. 3 as a function of propene incorporation. It can be seen, that there is a trend of decreasing heat of fusion, i.e. degree of crystallinity and melting point with increasing propene level, as expected. In the case of the melting point, a linear decrease is observed. These observations result from the random incorporation of an increasing amount of a disrupting co-unit,  $\text{CH}_2\text{-CH}(\text{CH}_3)\text{-C=O}$ , throughout the  $\text{CH}_2\text{-CH}_2\text{-C=O}$  polymer chain.

The crystalline density of the  $\beta$  phase was calculated (see Table 1), as described in the experimental section, from the experimentally determined cell parameters. The crystalline density decreases with increasing propene content. This is expected, and has been reported in polyethylene copolymers associated with a reduction in crystallinity and melting point [14]. The observed increase in unit cell parameters is mostly due to the expansion of the unit cell  $a$ -axis (see Table 1). Although this cell dilatation is partially related to the inclusion of some side-chains by some authors, it is usually associated with reduced lamella thickness [14]. Reduction in lamella thickness (suggested by a decrease in melting point) is thought to result in cell expansion due to surface dilatometric stresses, thermal vibrations and intracrystalline defects resulting from faster crystallisation at the large undercoolings required.

The crystalline density of the  $\alpha$  phase has also been determined using six reflections from the WAXS of the ECO film. This value is  $1.402\text{ g cm}^{-3}$  which is somewhat higher than the one reported in the literature [7,8], i.e.  $1.383\text{ g cm}^{-3}$ . The difference may arise from the fact that the value reported in the literature for the  $\alpha$  phase was measured in well-oriented polyketone fibers showing only

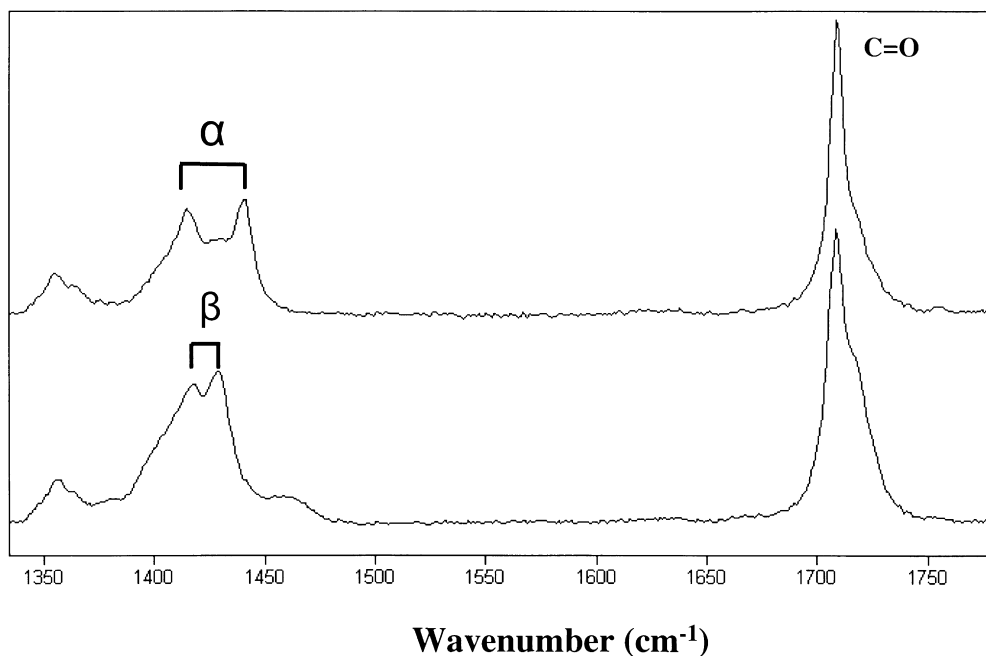


Fig. 5. Raman spectra in the range of 1325–1800  $\text{cm}^{-1}$  of (top) ex-reactor ECO with the largest content of  $\alpha$  form crystallinity and (bottom) ex-reactor EPCO(4.6) with only  $\beta$  form crystallinity.

the  $\alpha$  phase [7,8]. The fibers were obtained by solution spinning and subsequent hot drawing. Hence, the crystalline morphology is expected to be different and the average crystalline density could result in a lower value as it has been forced into the  $\alpha$  phase.

DSC measurements were also carried out on the samples characterised by WAXS to identify the  $\alpha$  to  $\beta$  phase transition reported [7,8] to occur around 100°C. This was only unambiguously detected for the ECO material (see Fig. 4). Although the WAXS pattern of EPCO(1.2) also shows a significant amount of  $\alpha$  phase (see Fig. 1 and Table 1), the phase transition was not observed by DSC. A proposed explanation is that the phase transition process may occur progressively in this sample over a wide range of temperature and the heat of transition is not observed as a sharp peak by DSC. This may suggest disperse irregular sized, thin and defected  $\alpha$  crystals. In the case of ECO, two close small endothermic peaks are seen, i.e. at ca. 85 and 105°C, which may suggest that there exist two types of  $\alpha$  crystal populations in this sample. Previous Raman work [9] showed that at a 100°C (around the phase transition temperature detected by DSC) the  $\alpha$  phase has partially disappeared for the ECO sample and that above this temperature only  $\beta$  phase is observed. Subsequent cooling down of this sample back to room temperature results in recovery of the  $\alpha$  phase. This therefore supports attributing the small DSC endotherms observed at about 100°C for ECO to a phase change in the crystalline morphology of the material. DSC did not detect an  $\alpha$  to  $\beta$  transition in the EPCO materials with higher propene contents, in agreement with the absence of  $\alpha$  crystals as characterised by WAXS.

### 3.2. Raman experiments

A previous study of aliphatic polyketones ex-reactor powder using Raman spectroscopy showed the potential of this technique for the elucidation of the structure and crystalline morphology of these family of materials [9]. Different Raman bands seen in the  $-\text{CH}_2-$  bending vibrational range of different materials, were assigned to the  $\alpha$  and  $\beta$  crystalline polymorphs proposed in the literature and discussed above (see Fig. 5). The presence of a band at 1440  $\text{cm}^{-1}$  was assigned to the  $\alpha$  form and thought to arise from a factor group splitting effect in the orthorhombic lattice similar to that observed for other polymers like polyethylene, polyoxymethylene, etc. [15]. On the other hand, the presence of a band at 1430  $\text{cm}^{-1}$  was attributed to the less packed distorted  $\beta$  form, this band was thought to arise from a weaker factor group splitting resulting in a smaller separation with the other component of the splitting, i.e. the band at 1415  $\text{cm}^{-1}$ . This band at 1415  $\text{cm}^{-1}$  is seen in all samples and it was tentatively assigned to the other component of the splitting for both polymorphs. Although, this band is slightly shifted towards higher wavenumbers in samples with  $\beta$  form, as a consequence of the reduction in the interchain interaction induced by higher lattice volume. The ECO polymer showed the three bands (1415, 1430 and 1440  $\text{cm}^{-1}$ ) pointing to a crystal phase mixture of both polymorphs, whereas EPCO polymers showed only two bands (1415 and 1430  $\text{cm}^{-1}$ ) suggesting a dominant  $\beta$  phase. This is exclusive above 2.9 mol% of propene [9]. The weak band at ca. 1460  $\text{cm}^{-1}$  was found to increase with increasing propene level in EPCO samples. This band is absent in

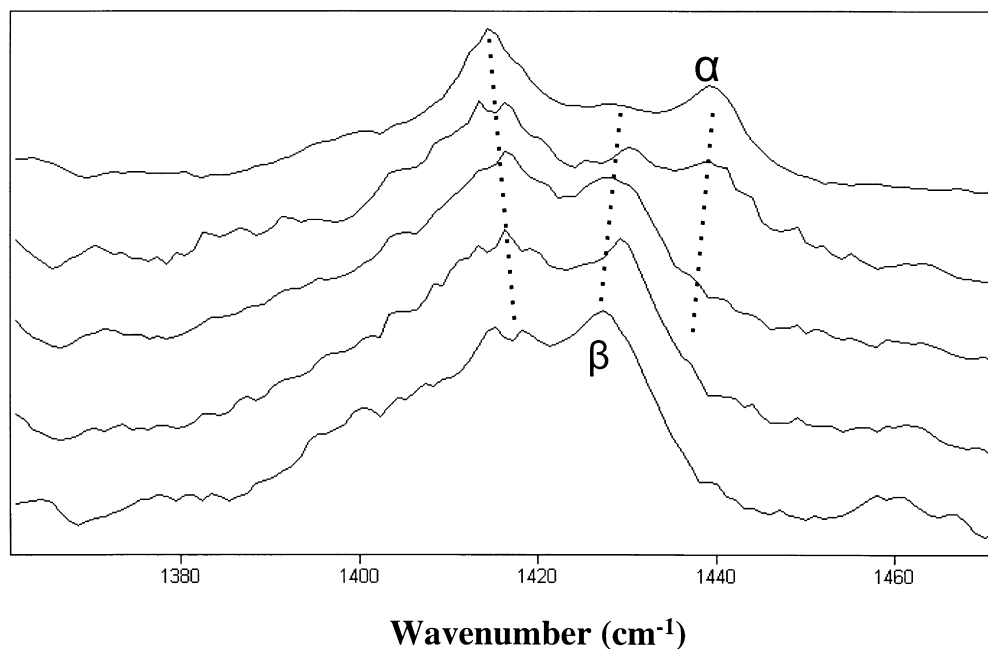


Fig. 6. Raman spectra in the range of 1360–1470  $\text{cm}^{-1}$  of film, from top to bottom, ECO, EPCO(1.2), EPCO(2.9), EPCO(4.6), EPCO(7.2).

the ECO polymer (see Fig. 5). As a consequence, this band was attributed to a  $-\text{CH}_3$  bending motion. Moreover, it compares well with the position of this mode in the Raman spectrum of polypropylene. A broad band can also be discerned at  $1410 \text{ cm}^{-1}$ . This band also develops with increasing propene level and is present in the ECO material. Consequently, it was attributed to the amorphous phase.

The Raman spectra, over the range of  $1360\text{--}1470 \text{ cm}^{-1}$ ,

of the compression moulded films, used for WAXS and DSC measurements, are shown in Fig. 6. The band at  $1440 \text{ cm}^{-1}$  assigned to the  $\alpha$  crystals is detected for ECO, EPCO(1.2) and very weakly for EPCO(2.9) samples, but not for the EPCO polymers with propene contents above 2.9 mol%. Consequently, the Raman ranking of the  $\alpha$  phase is seen qualitatively similar to that observed by WAXS in Fig. 1. A Raman method for the quantitative

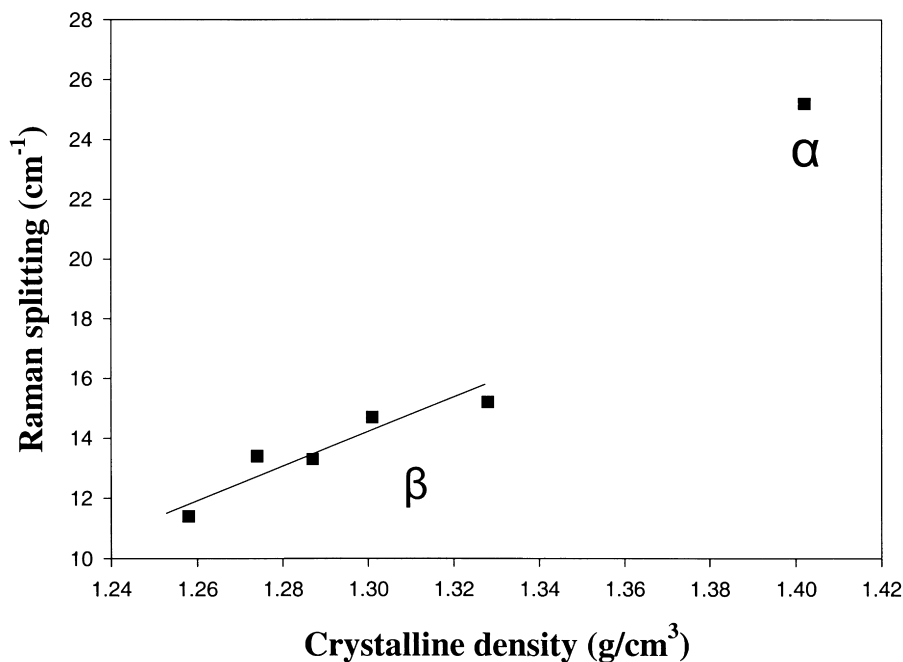


Fig. 7. Separation in wavenumber between the Raman  $\alpha$  and  $\beta$   $-\text{CH}_2-$  splittings versus the crystalline density as determined by X-ray for the various samples.

determination of the relative content of the  $\alpha$  to  $\beta$  phase is also proposed. This is derived (see column two in Table 1) by ratioing the area of the band at  $1440\text{ cm}^{-1}$ , attributed to the  $\alpha$  phase, to that of the C=O band arising at ca.  $1710\text{ cm}^{-1}$ . The mol% of C=O is always 50% throughout composition, therefore this band can be used as an internal standard for polyketones [9]. From Table 1, the relative  $\alpha$  phase Raman content (normalised to that in ECO) is found higher for EPCO(1.2) and slightly lower for EPCO(2.9) when compared to the WAXS data. The Raman method is anticipated to be more unreliable because of the extensive band overlapping seen in the  $-\text{CH}_2-$  bending range [9]. Moreover, the Raman signal in the films is relatively poor due to sample fluorescence.

The separation in wavenumber between the components of the  $\alpha$  ( $1440\text{--}1415\text{ cm}^{-1}$ ) and  $\beta$  ( $1530\text{--}1415\text{ cm}^{-1}$ ) factor group splittings was also measured for the various samples (see column five in Table 1). A general reduction of the  $-\text{CH}_2-$  bending splitting separation, i.e. a decrease in the lattice interchain interaction, is observed in the polyketone films with increasing propene level (see dotted lines in Fig. 6) in accordance with the observed cell expansion measured by WAXS (column three in Table 1). The fact that the cell expansion is mostly due to the enlargement of the  $a$  cell parameter, attributable to the lateral separation of the two interacting chains within the orthorhombic lattice, explains the marked change in splitting observed perpendicular to the chain direction  $-\text{CH}_2-$  bending vibrational mode. Fig. 7 shows that, there exists a reasonable linear correlation between the crystalline density of the  $\beta$  phase and the separation between the components of the  $\beta$   $-\text{CH}_2-$  bending splitting. However, this linear correlation does not seem to extend to the  $\alpha$  phase. The  $\alpha$  phase is known to have a slightly different chain arrangement within the lattice [7,8], and therefore results in a far more efficient interchain interaction, i.e. in a higher splitting separation, than the  $\beta$  phase. In accordance with this, a different dependence of the splitting separation with crystalline density may apply for the two polymorphs. Thus, although some variability was observed between the two methods proposed for the quantification of the  $\alpha$  phase, in general terms the agreement between Raman and WAXS data is good. This agreement makes both techniques suitable for the characterisation of the crystalline morphology present in aliphatic polyketones.

#### 4. Conclusions

WAXS, Raman and DSC showed a consistent picture of

the crystalline morphology, in terms of the  $\alpha/\beta$  polymorphism, present in a range of aliphatic polyketones. EPCO materials with propene level above 2.9 mol% exclusively showed  $\beta$  form, whereas the ECO polymer and the EPCO polymers below that content (2.9 mol%) showed a mixture of  $\alpha$  and  $\beta$  forms. Crystalline density and separation between the  $-\text{CH}_2-$  bending factor group splitting components (lattice interchain interaction) were found to correlate with each other, and decreased for both polymorphs with increasing propene level. This is consistent with the observed decrease in polymer heat of fusion (degree of crystallinity) and melting point. As expected, a deterioration of the crystalline morphology is caused by the random incorporation of propene, resulting in methyl side-chains, throughout the polymer chain.

#### Acknowledgements

Dr N.M. Dixon (BP Chemicals) is thanked for the Raman measurements. Mr P. Daniell (BP Chemicals) is acknowledged for supplying the samples. BP Chemicals is acknowledged for granting permission to publish this work.

#### References

- [1] Drent E, Budzelaar PHM. *Chem Rev* 1996;96:633.
- [2] Sommazzi A, Garbassi F. *Prog Polym Sci* 1997;22:1547.
- [3] Bonner JG, Powell AK. ACS meeting, San Francisco, 1997.
- [4] Bonner JG, Powell AK. *New Plastics '98*, London, 1998.
- [5] Chatani Y, Takizawa T, Murahashi S, Sakata Y, Nishimura Y. *J Polym Sci* 1961;55:811.
- [6] Chatani Y, Takizawa T, Murahashi S. *J Polym Sci* 1962;62:S27.
- [7] Lommerts BJ, Klop EA, Aerts J. *J Polym Sci Polym Phys* 1993;31:1319.
- [8] Klop EA, Lommerts BJ, Veurink J, Aerts J, Van Puijenbroek RR. *J Polym Sci Polym Phys* 1995;33:315.
- [9] Lagaron JM, Powell AK, Davidson NS. In preparation.
- [10] Mason SM, Conroy N, Dixon NM, Williams KPJ. *Spectrochim Acta A* 1993;49:633.
- [11] Langford JI, Louer D, Sonneveld EJ, Visser JW. *Powder Diffraction* 1986;1:211.
- [12] Balta-Calleja FJ, Vonk CG. *X-ray scattering of synthetic polymers*. Amsterdam: Elsevier, 1989.
- [13] Wilson ACJ. *J Sci Instrum* 1950;27:321.
- [14] Howard PR, Crist B. *J Polym Sci Phys* 1989;27:2269.
- [15] Bower DI, Maddams WF. *The vibrational spectroscopy of polymers*. Cambridge: Cambridge University Press, 1989.